Pergamon

Neuropharmacology 39 (2000) 2288–2301

NEURO PHARMACOLOGY

www.elsevier.com/locate/neuropharm

Postsynaptic hyperpolarization increases the strength of AMPA-mediated synaptic transmission at large synapses between mossy fibers and CA3 pyramidal cells

Nicola Berretta [a], Aleksej V. Rossokhin [b], Alexander M. Kasyanov [c, d], Maxim V. Sokolov [b, d], Enrico Cherubini [a,*], Leon L. Voronin [b]

[a] *Neuroscience Program and INFM Unit, International School for Advanced Studies, Via Beirut 2-4, 34014 Trieste, Italy*
[b] *Brain Research Institute, Academy of Medical Sciences, per. Obukha 5, 103064 Moscow, Russia*
[c] *Institute of Higher Nervous Activity and Neurophysiology, Russian Academy of Sciences, Butlerova Str. 5a, 117865 Moscow, Russia*
[d] *Leibniz Institute for Neurobiology, 39008 Magdeburg, Germany*

Accepted 13 April 2000

Abstract

In chemical synapses information flow is polarized. However, the postsynaptic cells can affect transmitter release via retrograde chemical signaling. Here we explored the hypothesis that, in large synapses, having large synaptic cleft resistance, transmitter release can be enhanced by electrical (ephaptic) signaling due to depolarization of the presynaptic release site induced by the excitatory postsynaptic current itself. The hypothesis predicts that, in such synapses, postsynaptic hyperpolarization would increase response amplitudes "supralinearly", i.e. stronger than predicted from the driving force shift. We found supralinear increases in the amplitude of minimal excitatory postsynaptic potential (EPSP) during hyperpolarization of CA3 pyramidal neurons. Failure rate, paired-pulse facilitation, coefficient of variation of the EPSP amplitude and EPSP quantal content were also modified. The effects were especially strong on mossy fiber EPSPs (MF-EPSPs) mediated by the activation of large synapses and identified pharmacologically or by their kinetics. The effects were weaker on commissural fiber EPSPs mediated by smaller and more remote synapses. Even spontaneous membrane potential fluctuations were associated with supralinear MF-EPSP increases and failure rate reduction. The results suggest the existence of a novel mechanism for retrograde control of synaptic efficacy from postsynaptic membrane potential and are consistent with the ephaptic feedback hypothesis.

Keywords: CA3 synapses; Retrograde signaling; Postsynaptic membrane potential; Ephaptic feedback; Failures; Quantal analysis

1. Introduction

Traditionally, chemical synaptic transmission has been considered to be polarized so that chemical synapses convey information in only one direction from the presynaptic to the postsynaptic cell. However, several forms of chemical retrograde signaling have been recently described (see Fitzsimond and Poo, 1998 for review). A novel form of retrograde signaling based on an electrical (or "ephaptic") rather than chemical mode of action has been proposed by Byzov (Byzov and Shura-Bura, 1986). We shall refer to this suggestion as the "ephaptic feedback hypothesis". It is assumed that, in purely chemical synapses, the excitatory postsynaptic current (EPSC) flowing through the extracellular space generates sufficiently strong depolarization of the presynaptic release site whenever the resistance of the synaptic cleft is high enough. The ephaptic feedback should be of positive sign in excitatory synapses. As with any positive feedback, this would amplify even small EPSP amplitude changes. A suitable amplitude increase can be achieved by postsynaptic hyperpolarization. Classically, postsynaptic hyperpolarization should enlarge AMPA-mediated postsynaptic response amplitude almost proportionally to the increase in the absolute value of the postsynaptic membrane potential due to an increased driving force for the ions mediating the current (Katz,

* Corresponding author. Tel.: +39-040-3787-223; fax: +39-040-3787-528 or +39-040-3787-249.
E-mail address: cher@sissa.it (E. Cherubini).

0028-3908/00/$ - see front matter
PII: S0028-3908(00)00076-9

1969). The increase should not be accompanied by changes in presynaptic transmitter release. In contrast, when a positive feedback of any kind (electrical or chemical) is present the amplitude increase should be "supralinear". In the case of the positive feedback according to the above ephaptic mechanism (Byzov and Shura-Bura, 1986; Voronin et al., 1995) the supralinear increase in EPSC or EPSP amplitude during postsynaptic hyperpolarization should be due to an enhancement in release probability. In apparent agreement with this prediction, it was found in a previous study (Voronin et al., 1999) that postsynaptic hyperpolarization reduced the failure rate and increased the quantal content of EPSCs/EPSPs recorded in the visual cortex and in the CA1 hippocampal area. However this effect was observed only in a minority of neurons during a strong (up to 40–60 mV) membrane hyperpolarization. Therefore it was not clear whether this mechanism would affect synaptic activity under physiological conditions.

According to the above hypothesis (Byzov and Shura-Bura, 1986) the positive feedback strongly depends on the resistance of the synaptic cleft. Therefore, it should be especially strong in large synapses with a long synaptic cleft. This prediction is specific for the ephaptic feedback hypothesis and is not evident for any chemical feedback. The mossy fiber (MF) endings, known to form large synapses onto the proximal dendrites at small electrotonic distance from the soma of CA3 pyramidal neurons (Claiborne et al., 1986) provide a suitable experimental model to test this prediction.

Therefore, the aim of the present study was to test the hypothesis of the ephaptic intrasynaptic feedback on the MF-CA3 synapses using a moderate artificial hyperpolarization (20 or 30 mV) and also by comparing EPSPs at different levels of spontaneous membrane potential fluctuations. We found increases in EPSP amplitudes larger than those expected from the changes in the driving force. The EPSP increases were associated with respective changes in several measures classically considered as indices of presynaptic transmitter release. The changes were especially strong for MF-EPSPs.

2. Methods

2.1. Slice preparation

Hippocampal slices were prepared from juvenile (7–18 days) Wistar rats (anesthetized with urethane, i.p. 10%) according to the method already described (Berretta et al., 1999). Slices were incubated at room temperature (18–22°C) in artificial cerebrospinal fluid (ACSF) of the following composition (in mM): NaCl 130, KCl 3.5, $CaCl_2$ 2, $MgCl_2$ 1.3, NaH_2PO_4 1.25, $NaHCO_3$ 25, D-glucose 11, L-glutamine 2 bubbled with 95% O_2 and 5% CO_2 (pH 7.4). Slices were individually transferred to a submerged recording chamber and continuously superfused with ACSF at 32–33°C. Picrotoxin (50 μM, Tocris Cookson Ltd, Bristol, UK) was routinely added to block $GABA_A$-mediated responses. (Alpha)-3-(2-carboxy-piperazin-4-yl)-propyl-1-phosphonic acid (CPP, 20 μM, Tocris Cookson Ltd, Bristol, UK) or D-2-amino-5-phosphono-pentanoic acid (AP5, 50 μM, Tocris Cookson Ltd, Bristol, UK) was present in most (75%) of the experiments to block NMDA receptors. A low concentration (5–10 nM) of tetrodotoxin (Affinity Research Products, Nottingham, UK) was also present in the perfusion medium to reduce polysynaptic responses and prevent epileptiform activity. Several experiments were made on young adult (4–6 weeks) rats with only a small variation in the recording conditions (Sokolov et al., 1998). The results obtained from both ages were similar and therefore the data were pooled.

2.2. Electrophysiological procedures

The whole-cell configuration of the patch-clamp technique was used to record EPSPs from CA3 pyramidal neurons (bridge mode) with an Axoclamp 2A amplifier (Axon Instruments, Foster City, CA, USA). Microelectrodes were pulled from thin-walled borosilicate capillaries (Clarke, Electromedical Instruments, Reading, UK). The pipette solution contained (in mM): K-gluconate 135, KCl 5, $MgCl_2$ 3, K_2ATP 2, HEPES 10 (pH 7.3 with KOH). The pipette resistance was 4–6 MΩ. Synaptic responses were evoked by alternate stimulation of the MF (electrode S-I or S-II in Fig. 1A) or the commissural/associative fibers (electrode CF in Fig. 1A) with pairs of stimuli (50 ms interval, 0.04–0.1 ms duration, 8–16 s between pairs) using bipolar twisted NiCr-insulated electrodes (50 μm, o.d.). The stimulus intensity was adjusted to induce minimal EPSPs with occasional failures to the first response. The membrane input resistance was monitored with −10 pA current pulses. After response stabilization, control paired synaptic responses (90–150 pairs) were recorded at resting membrane potential (from −55 to −65 mV). About the same number of responses were subsequently collected during 20 or 30 mV hyperpolarization below the resting. Data were digitized at 5 or 10 kHz. The membrane potential was measured in a 2 ms window just before each stimulus trial.

2.3. Response measurements and component analysis

To improve the signal-to-noise ratio and separate MF-EPSPs we used a covariance measure provided by the principal component analysis (Astrelin et al., 1998). Scores of the first principal component were determined from the initial slope and the peak. Such integral "covariance amplitudes" were strongly correlated with more common measures of peak amplitudes. They were

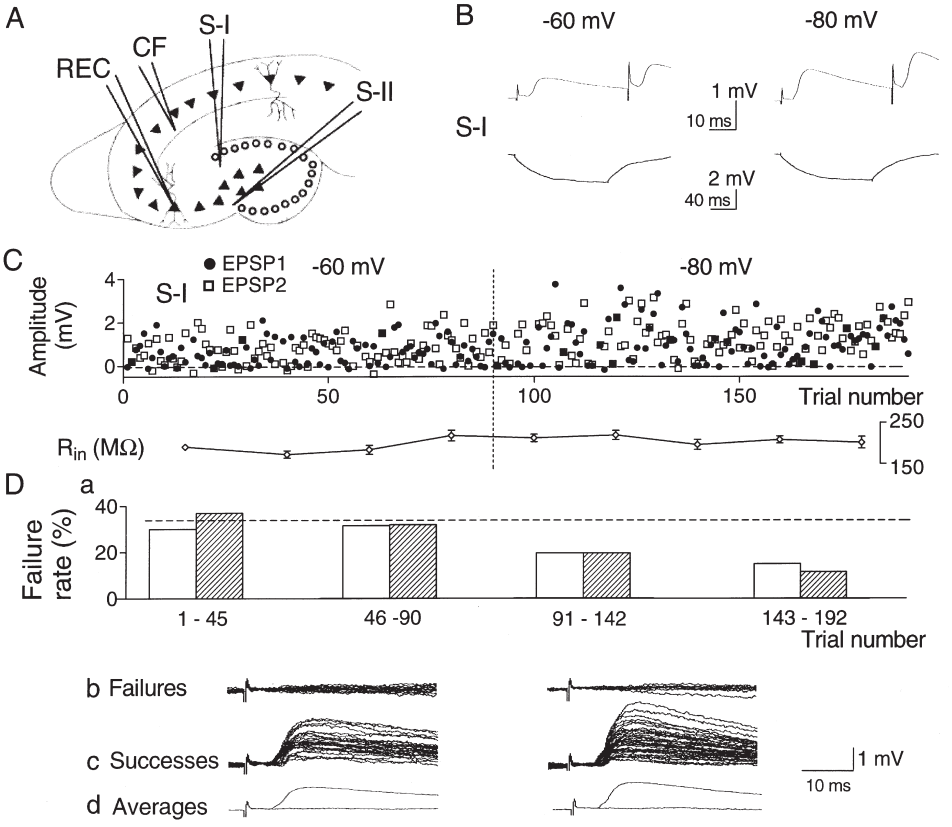

Fig. 1. Effects of postsynaptic hyperpolarization on MF-EPSPs. (A) Arrangement of recording (REC) and stimulating (CF, S-I, S-II) electrodes. (B) Averaged (n=90) EPSPs induced by stimulation via S-I electrodes at resting (−60 mV) and at hyperpolarized (−80 mV) membrane potential. The lower traces represent averaged (n=90) electrotonic potentials induced by −10 pA current steps. (C) Plots of EPSP amplitudes during repeated stimulation of the S-I input at 0.06 Hz. Dots and squares refer to EPSPs evoked by the first or second paired stimuli: EPSP1 and EPSP2, respectively. The graph R_{in} plots the mean membrane input resistance ±S.E.M. (n=30 for the first point; n=20 for other points). (D) a: Columns represent EPSP1 failure rates (N_0/N) plotted for the respective parts of the experiment. Open and hatched columns represent N_0/N determined by visual selecting failures and by doubling the number of negative amplitudes, respectively. The dashed line denotes the mean EPSP1 failure rate at −60 mV; it illustrates stability of the baseline N_0/N (compare trials 1–45 and 46–90) and similarity of N_0/N determined by the two methods (compare open and hatched columns). The difference in the failure rates (hatched columns) at −60 and −80 mV was significant ($P<0.05$, Chi-square test). b: EPSP1 failures; c: successes; and d: respective averages for the EPSP1 evoked by S-I stimulation (45 and 44 consecutive trials before and during hyperpolarization, respectively). Note a clear distinction between the smallest responses (c) and failures (b) as well as the flat averages for the visually-separated failures (d).

normalized to mV and are referred in the text as "amplitudes" for simplicity. The application of the component analysis allowed us not only to increase the signal-to-noise ratio, which is important for determination of failure rate and quantal analysis, but also to separate individual inputs from mixed EPSPs and thus to differentiate MF and CF inputs. The noise was measured for a window of the same duration (5–14 ms) taken before the stimulus artifact. To identify the response components (Fig. 2C, insets) we used the procedure described by Astrelin et al. (1998) according to which responses corresponding to positive values of one component and near 0 values of another component were averaged.

2.4. MF-EPSP identification

We used group II mGluR agonists and/or weak tetanization (100 Hz, for 1 s, three times at 20 s intervals with testing stimulus strength) to identify MF responses (Kamiya et al., 1996). The agonists were either DCG-IV ((2S,2′R,3′R)-2-(2′,3′-Dicarboxycyclopropyl)glycine), 1 μM or L-CCG-I ((2S,3s,4S)-CCG/(2s,1′S,2′S)-2-(Carboxycyclopropyl)glycine), 10 μM, both purchased from Tocris, Cookson Ltd., Bristol, UK. Because of technical difficulties related to the necessity of lasting recordings with infrequent (0.06–0.125 Hz) testing to avoid response rundown we did not perform the above tests for all recordings. Identification of the other inputs was based on the differences in the kinetics of the CF- and MF-responses used in the literature (Johnston et al., 1992). The rise time was measured from averages of at least 10 responses between 10 and 90% of their amplitudes. A criterion for the separation is given and justified in the Results. Altogether 15 cells were used in various experimental series, but only inputs with no statistically significant ($P<0.01$) amplitude drifts for at least 60 (up

to 150) consecutive control trials immediately before hyperpolarization were accepted for the basic analysis of the effects of hyperpolarization (n=16 MF-CA3 and 24 CF-CA3 inputs recorded from 13 neurons, see Results). Each cell was recorded from a separate slice so that the 15 cells were recorded from 15 different slices (14 rats). However data for one MF- and one CF-EPSP with very small control responses to the first pulse (EPSP1) before hyperpolarization ("presynaptically silent" synapses) were not included in the calculations where logarithms were calculated (e.g. Fig. 4A). To calculate the correlation coefficients, measurements from both EPSP1 and EPSP2 were used (Fig. 4A). Paired or unpaired t-tests or paired Wilcoxon test were used to assess the significance of differences, as appropriate. $P<0.05$ was taken as a significance level. The means are given together with their S.E.M. throughout the text.

2.5. Quantal analysis

To test the changes in the presynaptic release we used several approaches based on the quantal hypothesis of synaptic transmission (Katz, 1969). Firstly we used the failures analysis as the most illustrative approach. The number of failures (N_0) was estimated using two different methods: (i) Failures and successes were separated visually (Fig. 1Db, c). Averaging of failures and consideration of superimposed successes were used to control the separation (Fig. 1Dd). (ii) Failures were estimated as the double number of negative amplitudes (see Voronin, 1993). The similarity (Fig. 1Da) and high correlation between the failure rates (N_0/N) estimated by the two methods shown before (Voronin et al., 1999) and confirmed here (r=0.81, $P<0.0001$, 80 samples with at least 80 trials in each) indicate the adequacy of the visual selection. The data of Fig. 1D, Fig. 3D, Fig. 5C were obtained with both methods and those of Fig. 3C, Fig. 4A, Fig. 5D–G with the second one. We calculated N_0/N, percentage of its changes or changes in its logarithm ($\ln(N/N_0)$) at hyperpolarizing membrane potential relative to that at the resting. The value of $\ln(N/N_0)$ represents the mean quantal content (m) of the respective EPSP assuming the simplest release model based on the Poisson law (Katz, 1969). The statistical significance of N_0/N changes was assessed by applying the Chi-square test. As another simple approach, we used the variance analysis (see Voronin, 1993 for more details and Faber and Korn, 1991; Isaac et al., 1995 for reservations). We calculated the inverse squared coefficient of variation of EPSP amplitudes (CV^{-2}) which, similarly to $\ln(N/N_0)$ is equal to m for the Poisson release. To determine m without assuming any restricted model of the release process we estimated m more directly using a variant of the "unconstrained" noise deconvolution (see Astrelin et al., 1998 for Refs). Our algorithm searched for discrete distributions with coordinates x_i (distance from 0) and P_i (heights). The weighted mean interval between the bars was used to define quantal size (v) and m; 0.2 v was taken as intrinsic quantal variance (Astrelin et al., 1998; Larkman et al., 1997; Wall and Usowicz, 1998). This relatively small quantal variance corresponded to the respective estimate for presumed unitary MF-EPSPs (Jonas et al., 1993). Because stimuli had to be applied at a low rate (0.06–0.125 Hz) to diminish amplitude depression, the sample sizes were relatively small (185±5, n=80 amplitude distributions) even when we combined measurements from both responses in the paired-pulse paradigm. Computer simulations show that at the sample size of about 200, reliable estimates are obtained provided the ratio of v to the noise S.D. is >2.5. The mean ratio here was 3.7±0.1 (n=80). A strong correlation between v determined by the spectral (Fourier) analysis (Voronin, 1993) and by our computer algorithm (r=0.89, n=80, $P<0.0001$) confirmed the adequacy of our algorithm and of the suggested small intrinsic quantal variance for our case.

3. Results

3.1. Postsynaptic hyperpolarization increases amplitudes of minimal MF-EPSPs in a non-linear fashion and reduces their failure rate

Stimulating electrodes were placed either on the MF tract (S-I and S-II, Fig. 1A) to activate the mossy fibers or on the stratum radiatum to activate associative-commissural fibers (CF). Fig. 1B presents examples of averaged EPSPs elicited via S-I electrodes at the two membrane potential levels indicated. The −80 mV hyperpolarization was associated with a more than two-fold increase in the amplitude of the EPSP induced by the first pulse in the paired pulse paradigm. In this experiment, one could expect an increase of not more than one third of the control amplitude at −60 mV. This follows from the classical amplitude–voltage dependence with about 0 mV equilibrium potential (Katz, 1969) for the membrane potential shift from −60 to −80 mV. The input membrane resistance was not significantly changed during hyperpolarization or even decreased (Rin in Fig. 1B and C, see also Fig. 2B below and Section 3.2). Therefore, resistance changes could not explain the observed modifications of the EPSP amplitude. The trial by trial analysis (Fig. 1C) reveals one apparent reason for such "supralinear" amplitude increase: the postsynaptic hyperpolarization was associated with a reduction in the failure rate (Fig. 1D). The failure rate was calculated by separating failures visually (Fig. 1Da, open bars, Fig. 1Db) or by doubling the number of negative responses (Fig. 1Da, hatched bars). The visual estimates were controlled by averaging of all selected failures and successes (Fig. 1Dd). According to

both methods the failure rate was stable at −60 mV but decreased at −80 mV (Fig. 1Da).

3.2. Hyperpolarization effects are larger in MF- than in CF-inputs

Because of the extensive CF network (Johnston et al., 1992) stimulating electrodes placed on the MF tract can activate CF inputs also. Therefore, two different approaches were used to separate MF from CF inputs. First, a weak tetanus was delivered to afferent pathways in the presence of NMDA receptor antagonists (CCP or AP5, see Methods). This should produce a persistent potentiation of the MF- but not CF-EPSP (Johnston et al., 1992). Second, the effect of group II metabotropic glutamate receptor (mGluR-II) agonists on minimal evoked EPSPs was tested (DCG-IV or L-CCG-I in the presence of CPP). mGluR-II receptors are localized only on the MF and therefore their activation should reduce the MF- but not the CF-EPSPs (Kamiya et al., 1996). As shown in Fig. 2A, the EPSP elicited *via* the S-I stimulating electrode was strongly potentiated following a weak tetanus and suppressed by DCG-IV while the EPSP elicited by S-II stimulation was unaffected. Both properties identify the former EPSP as induced by MF activation. Moreover, consistent with non-MF properties (Bradler and Barrionuevo, 1990) a heterosynaptic NMDA-independent potentiation of the S-II-EPSP was observed following S-I stimulation (Fig. 2A, S-II). The above mentioned tests were performed on 24 EPSPs or EPSP components (see below) induced by S-I or S-II stimulation (altogether six cells from six slices). On the basis of these tests, nine inputs were identified as belonging to the MF and 15 inputs as to CF so that EPSPs or EPSP components mediated by both MF and CF inputs were recorded from all six cells. The rise time of identified MF-EPSPs varied from 1.2 to 4.4 ms, while that of the CF-EPSPs ranged from 1.9 to 8 ms. In addition, seven inputs activated with CF stimulating electrodes (Fig. 1A, CF) showed EPSPs with rise times ranging from 4.6 to 12 ms (five cells). Therefore, EPSPs induced via S-I or S-II electrodes having rise times >4.4 ms (from 5.1 to 11 ms, n=6) were a posteriori considered as CF-EPSPs. The slow kinetics of the non-MF EPSPs is in agreement with most reported data where differences in rise times were considered as the major criterion for the separation of MF and CF-mediated responses (Johnston et al., 1992, but see Henze et al., 1997).

Using a novel approach (Astrelin et al., 1998) based on the standard statistical techniques of the principal component analysis it was possible to separate EPSPs recorded in three cases into three distinct components having different latencies and rise times and 14 other cases into two components. An example is given in Fig. 2B–C, where two different components having different latencies could be clearly isolated from the EPSPs elicited with the S-I electrode. Fig. 2C plots the scores of the two components at −60 and −90 mV membrane potentials. Averaging the responses corresponding to positive scores of each component (with zero scores for the other one, within the fields delimited by the dashed boxes, Fig. 2C) produced wave forms (insets 1 and 2) with different latencies and rise times. Comparison of the component plots at −60 and −90 mV shows that the failure rate decreased during hyperpolarization: see the clusters around 0,0 coordinates comparable to the noise in the right hand plot. The decrease was due to changes in the second component with a faster rise time

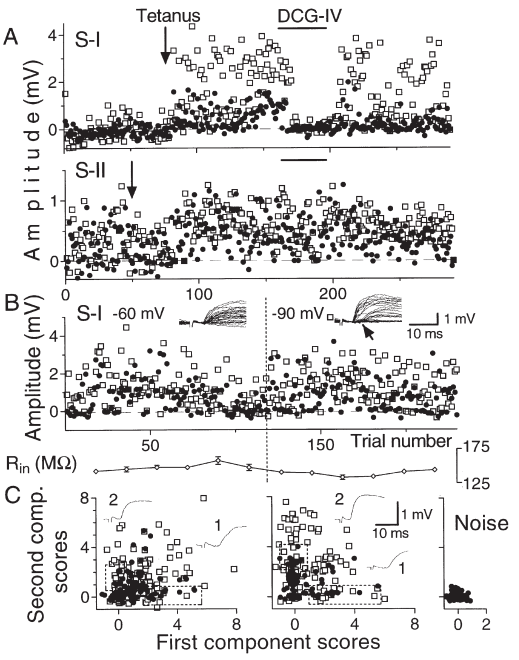

Fig. 2. MF-EPSP identification and component analysis. (A) Plot of the amplitudes of EPSPs evoked in the same neuron by stimulating via electrodes positioned at S-I or S-II sites (see Fig. 1A) before, during and after tetanization of respective pathways (arrows) and superfusion (bar) of the mGluR agonist (DCG-IV, 1 μM). Note homosynaptic long-term potentiation (LTP) in the upper plot, heterosynaptic LTP in the lower plot and depression of the S-I but not S-II evoked EPSPs during application of DCG-IV. Here and in B–C, dots and squares correspond to EPSP1 and EPSP2, respectively. The mean membrane input resistance was 389±10 MΩ (n=85), 349±9 MΩ (n=86) and 368±29 MΩ (n=35) during consecutive periods corresponding to control, post-tetanus and DCG-IV application, respectively. The input resistance slightly decreased after tetanus but did not change significantly following DCG-IV application supporting presynaptic effects of this drug selective for the MF input (Kamiya et al., 1996). (B) Similar amplitude plot from another experiment before and during membrane hyperpolarization. Insets show superimposed EPSPs. The oblique arrow denotes occasional longer latency EPSPs. The lower plot (R_{in}) represents the mean membrane input resistance calculated from 20 consecutive trials (±S.E.M.). (C) Component analysis of the EPSP from B. Scores of two components were obtained on the basis of the principal component analysis as described elsewhere (Astrelin et al., 1998). Insets 1 and 2 show averaged EPSP1 corresponding to respective dashed boxes (see Methods) and identifying fast (2) and slow (1) components. Note a stronger effect of postsynaptic hyperpolarization on component 2 whose faster rise time suggests MF activation.

(4.1 ms). This value was in the range of the rise time for identified MF inputs. The rise time of component 1 (6.5 ms) was outside this range. Therefore, the faster and slower components were considered to be mediated by the MF- and CF-inputs, respectively. With this type of analysis, six CF connections were dissected out from responses evoked with S-I or S-II stimulating electrodes. In the rest of the inputs, rise times were within the range of the identified MF-EPSPs (2.4–4.3 ms). As a result of all the above identification procedures, we identified 20 inputs as mediated by the MFs and 28 as mediated by the CFs (15 cells from 15 slices). The mean rise times (±S.E.M.) were 3.2±0.2 ms and 5.6±0.5 ms, for MF- and CF-EPSPs, respectively ($P<0.01$, *t*-test). Because the hyperpolarization effects were input specific rather than cell specific, our considerations are made in terms of inputs (or connections) rather than cells. The criteria for response stability (see Experimental Procedures) were fulfilled for 16 MF inputs (12 cells) and 24 CF inputs (12 cells) in experiments on 13 slice preparations from 12 rats.

In 12/16 MF inputs (10/12 cells) and in 10/24 CF inputs (7/12 cells) at resting membrane potential (−60 mV), the failure rate was at least 14% higher than that obtained at more hyperpolarized membrane potentials (−80 or −90 mV). These connections exhibited "supralinear" increases in their amplitudes. The summary data (Fig. 3A–B) show that in spite of the large variability of the hyperpolarization effect, the mean increase in the MF-EPSP amplitudes was larger than that expected from the classical voltage–amplitude dependence. The latter predicts at most only about 30 or 50% increases for hyperpolarization to −80 or −90 mV, respectively. In contrast, the mean increase in the CF-EPSP amplitudes was only slightly larger than that expected theoretically and was not statistically significant. The summary data for the failure rate (Fig. 3C–D) show a significant decrease in the failure rate during hyperpolarization in the MF, but not in the CF connections. Fig. 3E illustrates the above numerical difference in the distribution of hyperpolarization effects between MF and CF inputs (closed and open bars, respectively) representing the data as positive numbers: relative failure rate difference between more depolarized and hyperpolarized membrane potentials.

The input resistance of the recorded cells varied from 100 to 590 MΩ (on average it was 237±40 MΩ). In >50% of cases, the hyperpolarization was associated with a reduction in the membrane input resistance (Maccaferri et al., 1993), the average reduction being −26±6%. However, the reduction in input resistance did not correlate with the changes in failure rate ($r=-0.13$, $n=40$, $P>0.5$).

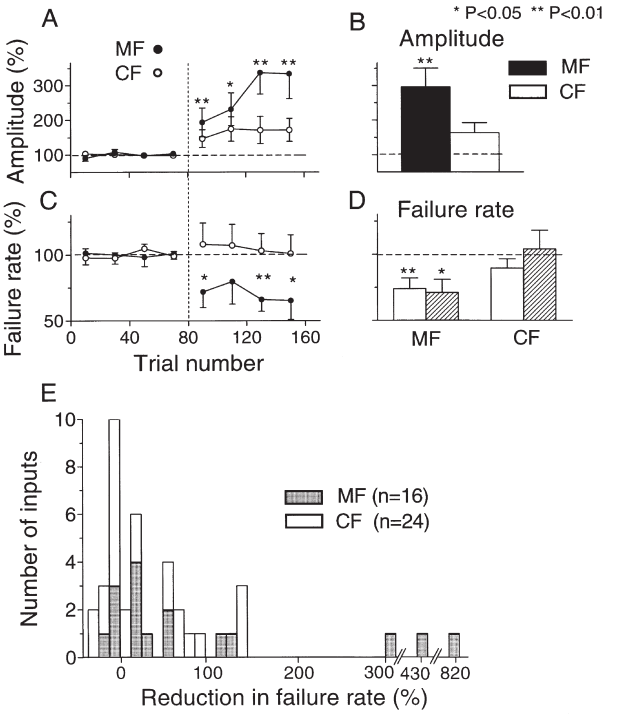

Fig. 3. Summary of the effects of hyperpolarization. (A) Summary changes in EPSP amplitudes for MF-CA3 and CF-CA3 inputs (closed and open circles, respectively) during repeated stimulation before and at the time of postsynaptic hyperpolarization (to the left and to the right of the vertical dashed line, respectively). Here and in B–D the data represent percentages of the mean values before hyperpolarization. The data were obtained from consecutive 20 trials for each input (±S.E.M.). Asterisks mark statistically significant differences from controls (at −60 mV, Wilcoxon test for matched pairs). (B) Summary data showing percent change of the EPSP amplitudes during hyperpolarization or MF-CA3 and CF-CA3 inputs (black and white bars, respectively). (C) Summary of failure rate changes during repeated stimulation before and at the time of postsynaptic hyperpolarization. The failure rate was determined by doubling the number of negative responses. (D) Summary of failure rate changes determined by visual inspection or as in C (open and hatched bars, respectively). The data here and in B include also available parts of recordings during hyperpolarization longer than shown in C and A, respectively. (E) Summary of the failure rate changes represented as distributions of differences in the failure rates during the resting membrane potential as compared to the hyperpolarized membrane potential. To express the failure rate (N_0/N) changes as positive values, the following formula was used $\{[(N_0/N)\text{dep}/(N_0/N)\text{hyp}]-1\}*100\%$, where (N_0/N)dep and (N_0/N)hyp are N_0/N at more depolarized (control) and more hyperpolarized membrane potentials, respectively. Eight black bars to the right from zero represent 12/16 MF inputs (10/12 cells, 10/12 slices) which showed >14% decrease in failure rate during postsynaptic hyperpolarization. Five black bars to the right of 100% show that the decrease was more than two-fold in five MF connections (5/12 cells).

3.3. Postsynaptic hyperpolarization changes indices of transmitter release

The summary plot of Fig. 4A presents relative changes in the amplitude of minimal evoked EPSPs versus failure rate (N_0/N) expressed as normalized $\ln(N/N_0)$. This value represents the mean quantal content (m) for

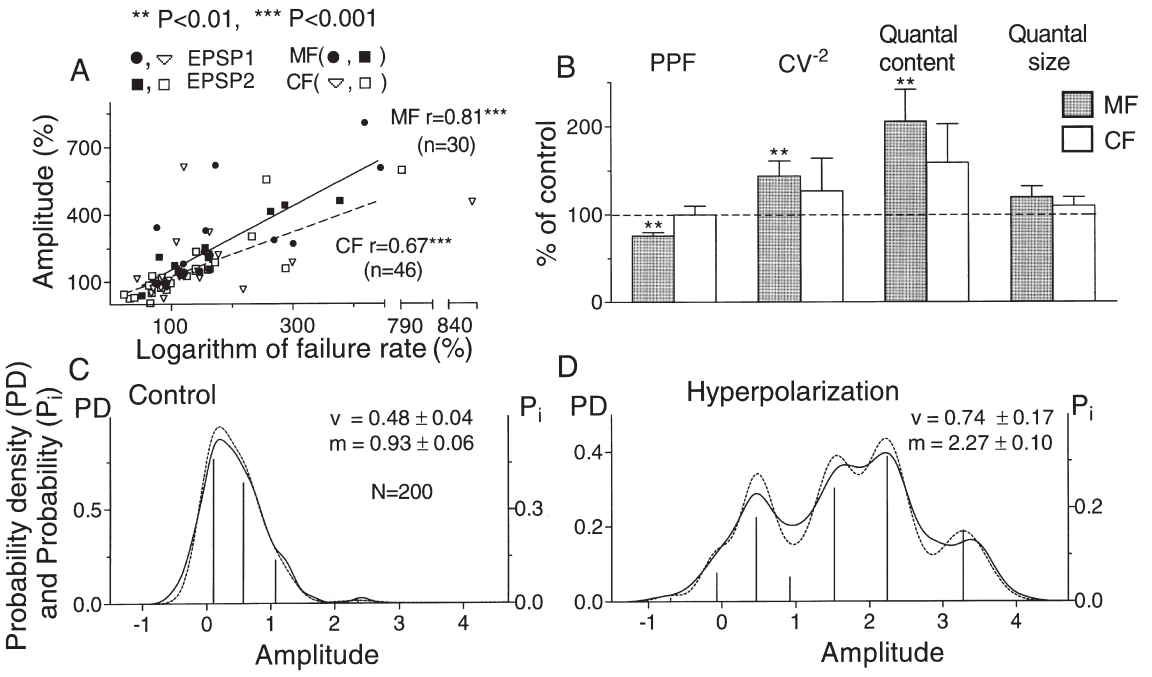

Fig. 4. Changes in indices of presynaptic release during hyperpolarization. (A) Correlation between changes in EPSP amplitudes and changes in $\ln(N/N_0)$. The values for the period during hyperpolarization for each input were expressed as the percentage relative to the control before hyperpolarization. The value of $\ln(N/N_0)$ which reflects the mean quantal content (m) for the Poisson model correlated with amplitude changes for both MF-CA3 (closed circles and squares) and CF-CA3 inputs (open triangles and squares). Note separate representation of the data for EPSP1 and EPSP2. Data for one CF and one MF input with very small control EPSP ("presynaptically silent" synapses) were excluded. Linear regression lines and respective correlation coefficients are given for pooled EPSP1 and EPSP2 measurements but separately for MF and CF inputs. (B) Summary changes in paired-pulse facilitation (PPF), inverse squared coefficient of variation (CV^{-2}), quantal content and quantal size for 16 MF and 24 CF inputs. One MF connection with small initial response amplitude was excluded from CV^{-2} calculations because the amplitude variance was smaller than the noise variance. For calculations of the quantal parameters based on the deconvolution techniques (see C–D) EPSP1 and EPSP2 amplitudes were pooled. Bars represent S.E.M., asterisks mark statistically significant differences from controls (at −60 mV). (C–D) Experimental (continuous curves) and predicted (dashed curves) amplitude distributions and deconvolved components (bars) found by the noise deconvolution procedure (see Astrelin et al., 1998) and used to estimate quantal size (v) and mean quantal content (m) in control conditions (C) and during hyperpolarization (D). Probability densities (left scales, PD) are for distributions; probabilities (right scales, Pi) are for bars.

the simplest (Poisson) model of transmitter release (Voronin, 1993). In the context of the classical quantal analysis the illustrated changes in $\ln(N/N_0)$ and their strong correlation with amplitude changes (Fig. 4A, r=0.81 for the MF inputs) indicate alterations in presynaptic release as a major cause of the amplitude increase. To further test this suggestion, additional parameters, traditionally considered as measures of transmitter release, were analysed. Firstly, we measured paired-pulse facilitation (PPF) which is a known presynaptic phenomenon (see Voronin, 1993 for reviews, but see Wang and Kelly, 1996). The PPF ratio for the MF input significantly decreased during hyperpolarization (Fig. 4B). However, the changes were not significantly correlated to amplitude alterations (r=−0.37, P=0.18, n=15). Secondly, we calculated changes in the inverse squared coefficient of variation of the response amplitude (CV^{-2}) which, similarly to $\ln(N/N_0)$, is equal to m for Poissonian release. Changes in CV^{-2} are also considered to reflect presynaptic modifications (Katz, 1969, but see Faber and Korn, 1991; Isaac et al., 1995). Fig. 4B shows a statistically significant increase in CV^{-2} for the MF connections. The increase correlated with amplitude modifications occurring during hyperpolarization (r=0.65, n=30, $P<0.001$, n=30, pooled data for EPSP1 and EPSP2). Finally, we determined m more directly using a variant of the noise deconvolution procedure (Astrelin et al., 1998). An example is shown in Fig. 4C–D. Note approximately equal (quantal) distances between the components of the deconvolution solution (Fig. 4C, bars), large changes in m, and a smaller increase in quantal size (v) during hyperpolarization (Fig. 4D). The average changes in m were significant for the MF inputs (Fig. 4B) and they correlated with changes in both EPSP amplitudes (r=0.76) and $\ln(N/N_0)$ (r=0.68, $P<0.001$, n=30). The small increase in v approximately matched the increase that could be theoretically expected. However the increase in v was not statistically significant (Fig. 4B), essentially smaller than the average amplitude increase and did not correlate with amplitude modifications. On average, CF connections showed a smaller EPSP amplitude increase during hyperpolarization (Fig. 3A, open circles), no significant changes in the failure rate (Fig. 3C, open circles), PPF ratio, CV^{-2} or m (Fig.

4B, open bars). Nevertheless, for cases with significant amplitude increases during hyperpolarization, $\ln(N/N_0)$ (Fig. 4A), CV^{-2} and m typically increased so that their correlation with amplitude changes was highly significant ($P<0.001$, $r=0.67$, 0.54 and 0.86, respectively, $n=46$). In summary, the above changes in the classical indices of transmitter release are compatible with presynaptic effects of postsynaptic hyperpolarization and with predominance of these effects in the MF input.

3.4. Spontaneous membrane potential fluctuations are associated with changes in failure rate

The question arises as to whether the changes in the failure rate represent a spurious phenomenon resulting only from relatively large (20–30 mV) artificial hyperpolarizations. Can they also be detected during smaller membrane potential fluctuations? To approach this issue, the failure rate was correlated with spontaneously occurring shifts in the membrane potential measured just before each stimulus trial. Fig. 5A plots membrane potentials (from the same experiment shown in Fig. 1) rearranged in ascending order, from more hyperpolarized to more depolarized values. Corresponding MF-EPSP amplitudes are plotted in Fig. 5B. It is clear from Fig. 5B–C that the number of failures was smaller during hyperpolarized membrane potentials as compared to depolarized ones. Although the reduction in the failure rate associated with spontaneous hyperpolarizations was statistically significant only in one case ($P<0.05$), it was observed in 15/16 MF connections (see Fig. 5G). Accordingly, the pooled data showed a significant change (Fig. 5D, MF, $P<0.001$, t-test for matched pairs here and below). The double hatched bar in Fig. 5D represents the mean membrane potential difference between the periods with "hyperpolarized" and "depolarized" membrane potentials as defined in Fig. 5A. The insets in Fig. 5B show that the amplitudes of the averaged EPSPs were also different between these periods, the mean difference for 16 MF connections (12 cells) was 46±19% ($P<0.02$). This value was about seven times larger than that predicted by the small changes in the EPSP driving force (Fig. 5D, double hatched bar). Reduced failure rate, associated with spontaneous hyperpolarizations was observed in 11/24 CF inputs with recordings from 8/12 cells. In three inputs (two cells) the changes were statistically significant ($P<0.05$). However, the pooled data showed no significant changes (Fig. 5D, CF) in spite of the significant difference in the membrane potentials between the respective periods (Fig. 5D, CF, double hatched bar). Accordingly, there was no significant difference between the mean EPSP amplitudes for the hyperpolarized and depolarized periods in the CF inputs (10±19%, $n=24$, $P>0.5$).

As a control for the failure rate changes in the MF connections during spontaneous membrane potential fluctuations, the same recordings were divided into two equal parts before sorting (30 to 63 trials). No significant differences in the failure rate ($P>0.4$) or the mean membrane potential ($P>0.1$) were found between the two parts (Fig. 5E). As an additional control, failure rates were related to the membrane potential measurements done on a trial applied 3 min before (Fig. 5F). There was no significant difference between the respective failure rates ($P>0.79$) in spite of a significant membrane potential shift (Fig. 5F, double hatched bar). The control procedures (Fig. 5E–F) indicate that the effect of membrane hyperpolarization on MF-EPSPs (Fig. 5D) was not fortuitous. In addition, a strong correlation was observed between changes in $\ln(N/N_0)$ during spontaneous and during artificial hyperpolarization (Fig. 5G). Even a slightly larger correlation was observed when the failure rate rather than its logarithm was used ($r=0.83$, $P<0.001$, $n=16$ inputs, 12 cells). No similar correlation was found for the CF inputs ($r=0.04$ for the failure rate and $r=0.18$ for its logarithm, $P=0.86$ and 0.43, respectively, $n=24$). We did not apply the deconvolution analysis to study the effects of spontaneous membrane potential shifts because of small effects and sample sizes. However, statistically significant changes in $\ln(N/N_0)$ ($P<0.01$, see Fig. 5G, ordinate), CV^{-2} (55±24% increase during hyperpolarization, $P<0.05$) and PPF ratio (12±6% decrease, $P<0.01$) supported an increase in transmitter release.

4. Discussion

4.1. Novel experimental observations

The major results of our experiments demonstrate a novel effect of postsynaptic hyperpolarization, i.e. a large increase in the EPSP amplitude. We stress the following points: (i) the increase was stronger than that predicted from the shift in the driving force; (ii) it was associated with changes in several parameters classically considered to represent indices of presynaptic transmitter release; (iii) the effects were especially strong during recordings of the EPSPs evoked by stimulation of presumed mossy fibres mediated by large synapses having large synaptic cleft with high resistance; (iv) the effects were weaker on the EPSPs induced via activation of putative associative-commissural fibres (present data) or on neocortical and CA1 EPSPs and EPSCs (Voronin et al., 1999) induced by activation of smaller synapses with smaller resistance of the synaptic cleft. Superficially, these observations seem to contradict published experimental data because no deviations from linear amplitude–voltage relationships have been reported with recordings of EPSCs from various structures including the CA3 hippocampal area (e.g. Jonas et al., 1993; Urban

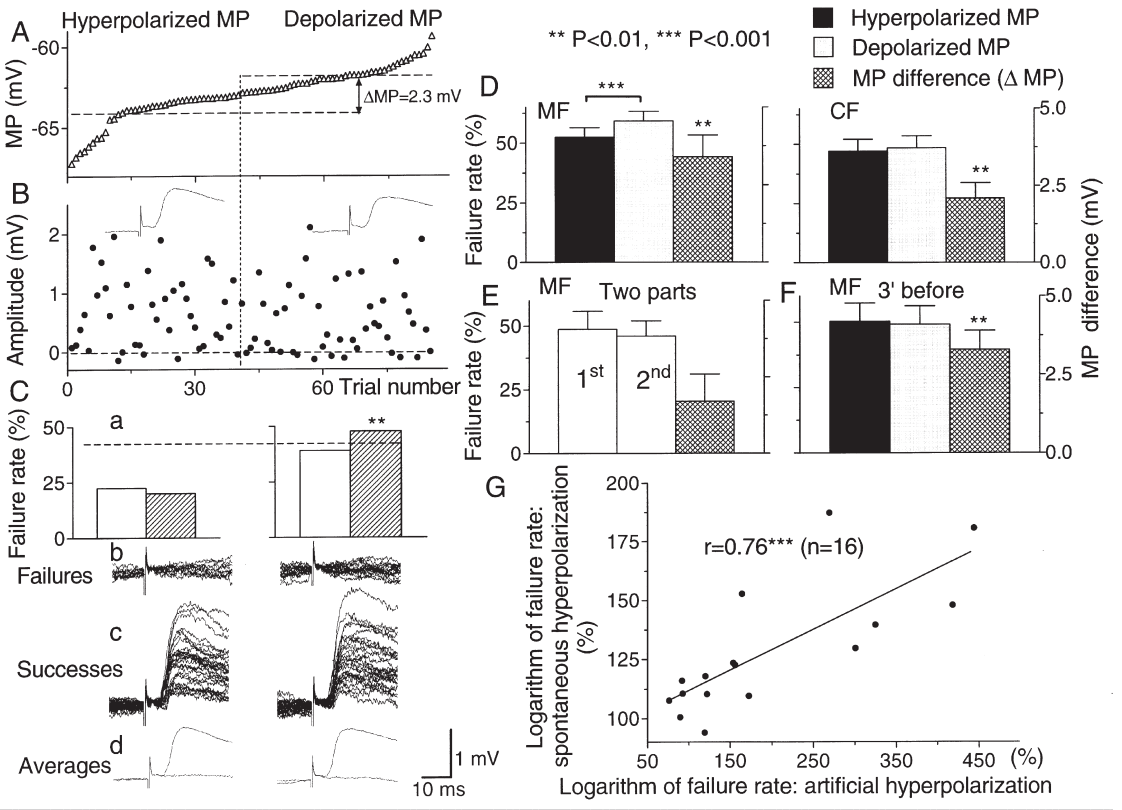

Fig. 5. Failure rate changes during spontaneous membrane potential fluctuations. (A) Membrane potential values sorted in the ascending order from more hyperpolarized to more depolarized values (same experiment shown in Fig. 1C). Vertical dashed line shows the mean membrane potential over the whole period; horizontal dashed lines show the mean membrane potential values for periods to the left and to the right from the general mean ("Hyperpolarized MP" and "Depolarized MP", respectively). ΔMP=2.3 mV represents the difference between the mean membrane potentials for these two periods. (B) Plot of MF-EPSP amplitudes corresponding to the membrane potential values in A measured immediately before each stimulus. The insets represent averages over the respective periods. Note the smaller average and larger number of small amplitudes (presumed failures) at more depolarized membrane potential (to the right of the vertical dashed line). (C) Failure rates (a) determined in the same experiment by visual selecting failures and by doubling the number of negative amplitudes (open and hatched columns, respectively) given separately for the hyperpolarized (left) or depolarized (right) membrane potentials. (b–d) Failures (b) and successes (c) separated visually and superposition of their averages over respective periods (d). See Fig. 1 for other explanations. Asterisks mark statistically significant differences between the two periods. (D) Failure rates during hyperpolarized and depolarized periods of spontaneous membrane fluctuations (black and gray columns). The number of inputs: 16 (12 cells) and 24 (12 cells) for MF and CF, respectively. The double hatched bars give average membrane potential differences between depolarized and hyperpolarized periods (see ΔMP in A). Here, in control measurements (E, F) and for G, the failure rate was determined by doubling the number of negative amplitudes. The asterisks denote the significant difference between the two periods (D, dots above the horizontal bar) or significant differences from 0 (D and F, asterisks above the double hatched bars, *t*-test for matched pairs). (E) Failure rate during two equal parts (1st and 2nd) of the same recordings used in D but without sorting the trials according to the membrane potential levels. (F) Failure rates (MF-CA3 inputs) for two parts sorted according to the membrane potential measured 3 min before each stimulus (black and gray columns) and respective membrane potential difference (double hatched bar). Note significant differences in D (MF) and no differences either for the CF inputs (D) or for the MF inputs in the control procedures (E–F). (G) Dependence between failure rate changes resulted from spontaneous and induced hyperpolarizations in the same neurones (data for 16 MF inputs). Linear regression line and the coefficient of the correlation (r) are shown.

and Barrionuevo, 1998). No changes in indices of transmitter release of AMPA mediated EPSCs (e.g. PPF, see Clark et al., 1994) have been reported previously. The deviations cannot be explained by differences in the recording procedures because we observed similar supralinear changes in voltage-clamp experiments on minimal EPSCs (Voronin et al., 1999 and our unpublished observations at CA3 area). Our recent computer simulations and experimental data suggest that the major reason for this apparent discrepancy is that composite rather than minimal responses have been evoked in previous studies (Clark et al., 1994; Jonas et al., 1993; Urban and Barrionuevo, 1998). Our unpublished observations suggest that activation of adjacent synapses would counterbalance the unusual effects of postsynaptic hyperpolarization, making the amplitude–voltage relationship linear for composite EPSCs. There are two major reasons for such an effect. First, a strong stimulation used to induce composite responses activates multiple inputs, including those not endowed with positive feedback. The resulting summation of non-linear and linear relationships would decrease the non-linearity. Second, additional synapses, especially remote ones, can be imperfectly clamped and therefore can produce depolarizing postsynaptic currents

which can counterbalance the artificial postsynaptic hyperpolarization applied via somatic microelectrode.

To better understand the unusual effects of postsynaptic hyperpolarization on minimal excitatory responses, we shall discuss the hypothesis of the ephaptic feedback, which allows us to predict the above effects as well as the difference between the effects on MF and CF inputs.

4.2. Intrasynaptic ephaptic feedback hypothesis

Our experiments were designed to test the hypothesis of A.L. Byzov (Byzov and Shura-Bura, 1986) on the existence of a positive ephaptic feedback in purely chemical synapses.

One consequence of the feedback is that postsynaptic hyperpolarization which is known to increase the postsynaptic current through the increase in driving force would cause a larger increase of the EPSC. The larger increase is due to additional transient ephaptic depolarization of the presynaptic terminal produced by the increased EPSC itself. This additional depolarization would lead to enhanced transmitter release. The simplified electrical scheme (Fig. 6) illustrates how the additional ephaptic depolarization is created. The scheme shows pre- and postsynaptic sites with respective input membrane resistances (*R1* and *R2*) and resting MPs (*E1* and *E2*). The resistance of the presynaptic ending (*Rp*) is shown separately. The continuous arrow *Is* represents the EPSC generated by opening of subsynaptic ion receptor channels (variable resistance *Rs*). The current creates a potential drop *Vg* across the synaptic gap resistance *Rg* (− and + below *Rg*). The negative potential (point 3) relative to the extracellular compartment (point 4) should depolarize the releasing site and therefore increase Ca^{2+} influx into the presynapse (arrow at the left). This may enhance transmitter release thus creating a positive intrasynaptic feedback. This type of linking differs from electrical coupling via specialized gap junctions and can be called “ephaptic”. Another physically equivalent explanation of the feedback considers an additional return path for *Is* (Fig. 6, dashed arrow). This current branch would hyperpolarize parts of the presynapse remote from the synaptic release site (+ and − over *R1*) but depolarize the presynaptic membrane (Takeuchi and Takeuchi, 1961). The depolarization will be the largest at the place of the transmitter release (+ and − over *Rp*) and therefore can additionally increase transmitter release during EPSC if strong enough.

Therefore the ephaptic feedback adds a fast depolarization to that produced by the presynaptic spike. The major presynaptic Ca^{2+} influx is known to take place during the falling phase of the presynaptic action potential (e.g. Sabatini and Regehr, 1999). That is why broadening of the presynaptic spike is so effective in increasing release probability (Jackson et al., 1991; Byrne and Kandel, 1996). Thus, any additional depolarization occurring during presynaptic action potential repolarization should be effective in increasing release probability, being somewhat analogous to presynaptic spike broadening.

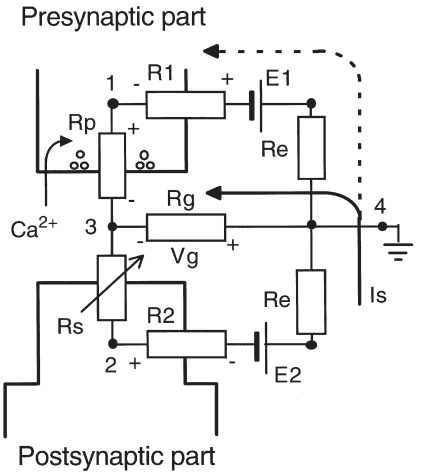

Fig. 6. Simplified electrical scheme of the chemical synapse to illustrate ephaptic feedback. Activated synapse with the resistances of the subsynaptic receptor membrane (*Rs*), of the release site of the presynaptic membrane (*Rp*), input resistances (*R1* and *R2*) of the pre- (point 1) and postsynaptic (point 2) sites, batteries (*E1* and *E2*), representing respective resting membrane potentials and the resistance of the synaptic gap (*Rg*). Resistances of extracellular space (*Re*) are shown but they can be ignored because they are negligible in comparison with other resistances. The continuous arrow *Is* shows the direction of the EPSC which creates a potential drop *Vg* on the resistance of the synaptic gap (*Rg*) which is negative at the center of the synaptic gap (− at point 3) relative to the extracellular space (+ at point 4). The positive feedback is created by the negative *Vg*, which is applied close to the locus of transmitter release. This would induce a depolarization of the presynaptic release site, increased Ca^{2+} influx (left-hand arrow) and additional transmitter release during EPSC generation. The dashed arrow illustrates another (equivalent) explanation of the positive ephaptic feedback showing a component of Is passing through the presynaptic part and thus depolarizing the release site (+ and − over *Rp*).

We used the simplest scheme with a single release site to simplify the feedback illustration. Recent recordings from putative single synapses at CA1 demonstrated a strong suppression of EPSCs evoked at short intervals suggesting a short-term synaptic depression after a prior exocytotic event (Dobrunz et al., 1997). This observation seems to contradict the intrasynaptic ephaptic feedback hypothesis that supposes additional transmitter release immediately after EPSC generation. More detailed considerations (Voronin et al., 1995 and unpublished simulations) show that the ephaptic feedback mechanism is applicable to synapses with multiple release sites similar to giant MF-CA3 synapses. In such synapses, additional presynaptic depolarization increases transmitter release from adjacent release sites provided that *Rg* is high enough. Accordingly, for a junction with multiple release sites no depression was found at short intervals following previous release (Winslow et al., 1994).

Theoretically, the failure rate under our conditions

could also be influenced by "artefact" (or artificial) failures, which can occur from: (i) the failure to excite the presynaptic fibre by the stimulating electrode ("stimulation failure") or (ii) the failure of the presynaptic spike to induce sufficiently strong depolarization at the release site ("invasion failure"). Such artificial failures can be sensitive to presynaptic conditions. However, most of the presynaptic axon would be hyperpolarized rather than depolarized during postsynaptic hyperpolarization in a synapse with ephaptic feedback (Fig. 6, dashed arrow, signs − and + over *R1*). Therefore, the axon excitability would tend to decrease rather than increase although this hyperpolarization should be negligible, especially under the stimulating electrode remote from the presynaptic ending. In any case, the number of "stimulation failures" is not expected to decrease. Possible changes in the number of "invasion failures" would strongly depend on the geometry of the presynaptic ending and distribution of voltage-dependent channels. Testing this will require a special study. Theoretically this mechanism could contribute to the effects of the postsynaptic hyperpolarization in synapses with the ephaptic feedback. However, under our conditions the number of "artificial failures" of both types seems to be negligible given that the average amplitude of the facilitated second response in the paired-pulse paradigm did not depend on whether it followed response failures or successes (unpublished observations, see also Voronin et al., 1992 for similar data in CA1). In fact, in the case of failure of presynaptic spike invasion, no presynaptic PPF should be observed.

In Fig. 6, the critical parameter is *Rg*. It determines *Vg* magnitude and therefore the strength of the positive ephaptic feedback. Approximate *Rg* evaluations (Byzov and Shura-Bura, 1986) have shown that the feedback is negligible in small flat synapses with a diameter of about 0.3 μm. However it should be strong enough in synapses with thin (e.g. 0.2–0.4 μm) postsynaptic processes (spinules) invaginating into presynaptic terminals for >1 μm. Such conditions are met in case of the giant MF synapses of up to 4–6 μm in diameter (Claiborne et al., 1986). Our unpublished evaluations showed that additional presynaptic depolarization due to the ephaptic feedback can reach >50% of the EPSP amplitude. In contrast, CF synapses are typically smaller and therefore have smaller synaptic cleft resistance. The differences in synaptic cleft resistance may explain the observed diversity of the effects of the postsynaptic hyperpolarization on MF and CF inputs. Therefore this diversity supports the ephaptic feedback hypothesis.

4.3. Alternative explanations

Although the intrasynaptic ephaptic feedback hypothesis explains our experimental data satisfactorily, other possibilities can not be excluded. Theoretically several pre- and postsynaptic effects of postsynaptic hyperpolarization could produce apparently supralinear amplitude increases. Each such mechanism can be considered as a feedback from the postsynaptic membrane potential. The reverse is not true, i.e. not all types of a positive feedback would lead to non-linear increases in the EPSP amplitude with hyperpolarization. Therefore our data limit a range of possible feedback mechanisms. For example, the changes in presynaptic release during or following postsynaptic manipulations, such as those described in the Purkinje cell of the cerebellum (Glitsch et al., 1996) or in CA1 pyramidal cells (Bliss and Collingridge, 1993) are explained by the release of chemical retrograde messengers (Fitzsimond and Poo, 1998). However, these substances as well as ions such as Ca^{2+} or K^+ (Takeuchi and Takeuchi, 1961) are proposed to be secreted by postsynaptic depolarization and not by hyperpolarization and therefore their release is expected to be suppressed by hyperpolarization. To fit our data, postsynaptic hyperpolarization should either suppress the release of an inhibitory chemical messenger tonically secreted by the postsynaptic cell at rest (Voronin et al., 1999) or increase its uptake by the postsynaptic cell. A hypothetical possibility could be glutamate (Glitsch et al., 1996) acting on inhibitory presynaptic receptors. However the possibility of presynaptic metabotropic glutamate receptor is unlikely because the metabotropic glutamate receptor antagonist MCPG did not significantly change baseline amplitudes of minimal MF-EPSPs and failed to prevent the unusual effects of postsynaptic hyperpolarization (Gasparini, Cherubini, Kasyanov and Voronin, unpublished observations). Involvement of inhibitory presynaptic ionotropic receptors is more difficult to test. However, facilitating after-effects of intracellular depolarization in several types of synapses (see Voronin et al., 1995 with Refs) including the MF-CA3 synapse (Berretta et al., 1999) are difficult to reconcile with this possibility.

Theoretically, changes in response amplitudes, failure rate, CV^{-2} and quantal content during hyperpolarization might be attributed to several potential postsynaptic mechanisms which are listed below (e.g. Isaac et al., 1995; see also Voronin et al., 1999).

(i) Low amplitude (below noise level) responses could have increased and become measurable. However, according to the classical linear amplitude–voltage dependence with about 0 mV reversal potential, known for the MF input, artificial somatic hyperpolarization for 20 or 30 mV should produce <50% increase in the EPSP amplitude. The increase would be even smaller during spontaneous membrane potential fluctuations. This could not explain the appearance of responses such as those illustrated in Fig. 1Dc and Fig. 5Cc (compare with failures in Fig. 1Db and Fig. 5Cb, respectively). To convert previously invis-

ible responses to measurable ones, their amplitude should increase at least several fold, compatible with a positive feedback mechanism. We stress that the classical explanation based on changes in the driving force is also clearly incompatible with other reported findings additional to changes in the failure rate: supralinear increases in the MF-EPSP amplitude, changes in their distribution and modifications of other indices of transmitter release.

(ii) New AMPA type ionotropic glutamate receptor (GluR) clusters could have been exposed, as has been suggested for NMDA dependent LTP induced by postsynaptic depolarization in CA1 (Isaac et al., 1995; Durand et al., 1996). However in the present experiments, the postsynaptic membrane was hyperpolarized and not depolarized. There is no evidence for such a mechanism in numerous studies of the voltage dependencies of AMPA receptor currents recorded from pyramidal neurons (Jonas and Burnashev, 1995) including a study on patches from dendrites of CA3 pyramidal neurons (Spruston et al., 1996). In addition, a postsynaptic mechanism would be difficult to reconcile with a reduction in the PPF ratio.

(iii) Increased activity of voltage-dependent channels could evoke supralinear changes in EPSP amplitudes. The most likely candidate is the low-threshold Ca^{2+} current, or T current (Huguenard, 1996) whose inactivation could be reduced by hyperpolarization. However, several lines of reasoning argue against this explanation. Voltage-dependent channels were shown to be activated only when composite EPSPs reached about 20 mV amplitude (Markram and Sakmann, 1994) and they contributed to the EPSP peak rather than to its initial slope. Therefore this mechanism could hardly explain the non-linear increases in minimal EPSP amplitude observed in our experiments as well as changes in the failure rates, PPF and amplitude distributions with lack of significant changes in the estimated quantal size. An even stronger argument against this possibility is that non-linear effects of postsynaptic hyperpolarization were also observed under voltage-clamp conditions (Voronin et al., 1999 and our unpublished observations at CA3) when the voltage-dependent activity should be strongly suppressed.

The intrasynaptic ephaptic feedback hypothesis explains satisfactorily all of our basic findings: supralinear EPSP amplitude increases during postsynaptic hyperpolarization, significant hyperpolarization effects on indices of transmitter release and different effects on the MF and CF inputs. In fact, it is expected that in comparison with giant MF synapses, the CF synapses have smaller *Rg*, weaker ephaptic feedback and therefore, on average, smaller hyperpolarization effects. Accordingly, the strength of the hyperpolarization effects on the CF-EPSP is similar to the effects on the EPSPs evoked by Schaffer collateral stimulation in CA1 hippocampal neurons (Voronin et al., 1999). The more pronounced effects on MF- as compared to CF-responses could be partially explained by the more proximal location of the MF-CA3 synapses especially under voltage-clamp because of different clamping conditions. However, all present experiments were performed under current clamp. Simulation studies have shown that attenuation of the constant current along the dendrite is small (Spruston et al., 1994). According to a classical view (see e.g. Wu and Saggau, 1997) a steady presynaptic membrane depolarization may increase spontaneous release and suppress the evoked one. The depression of the evoked release may be due to a decrease in presynaptic spike amplitude following inactivation of Na^+ or/and Ca^{2+} channels. However, local depolarization at the releasing site may also essentially increase release probability due to several mechanisms (Wu and Saggau, 1997). Also the inactivation can be only partial and therefore the depolarization can increase the presynaptic Ca^{2+} level and be accompanied also by calcium-induced Ca^{2+} release.

4.4. Physiological implications

An important observation is that highly non-linear changes in the EPSP amplitude associated with changes in failure rate, CV^{-2} and PPF could be revealed not only during relatively large artificial hyperpolarizations but also during spontaneous membrane potential fluctuations. In principle, the underlying mechanisms could be different from those triggered by artificial hyperpolarization. For example, some common factors may influence both the membrane potential and presynaptic release. However, the high correlation between failure rate reduction during spontaneous and artificial hyperpolarizations is compatible with the hypothesis that both phenomena are accounted for by the same mechanism, presumably the ephaptic intrasynaptic feedback. Some deviations from the expected dependence between the effects of spontaneous and artificial hyperpolarizations could be due to statistical fluctuations of N_0/N and differences between somatic and dendritic membrane potential levels attained under two different conditions. The latter argument can be especially relevant to the remote CF synapses.

Our experiments show strong (supralinear) changes in EPSP amplitudes and in indices of transmitter release. In spite of possible different interpretations of the present results i.e. whether the reported modifications are mediated ephaptically or chemically or whether they are localized pre- or postsynaptically, our data strongly suggest the existence of a novel form of retrograde communication in central synapses. The correlation between spontaneous membrane potential fluctuations and failure rates indicates that this novel type of feedback can con-

stitute a mechanism for effective operative control of presynaptic transmitter release from single synapses by the ongoing postsynaptic membrane potential changes which are known to be particularly prominent in vivo.

The physiological significance of this novel feedback may consist not only in the retrograde control but also in amplification of signals from a subset of synapses, for example in response to "modulatory" transmitters, which are known by their common postsynaptic hyperpolarizing action. The subset includes large synapses as well as synapses that have increased their size following plastic reorganizations or acquired spinules and invaginations, factors which would increase synaptic cleft resistance. Structural modifications have been reported after LTP induction (see Edwards, 1995; Muller, 1997) and memory formation (Calverley and Jones, 1990). One implication of the positive intrasynaptic feedback is that any postsynaptic mechanism that increases postsynaptic current would also influence presynaptic release. This could contribute into solving the lasting debate on pre- and postsynaptic maintenance mechanisms of LTP (Bliss and Collingridge, 1993; Edwards, 1995; Voronin et al., 1995). The positive intrasynaptic feedback may explain apparent release synchronization revealed by spontaneous multiquantal releases (Korn et al., 1993; Wall and Usowicz, 1998) and by large "all-or-none" responses (Volgushev et al., 1995; Stratford et al., 1996).

Summarizing, the above findings were obtained in experiments designed to test Byzov's hypothesis on ephaptic intrasynaptic feedback (Byzov and Shura-Bura, 1986). We found no clear contradictions between the hypothesis and our data and those found in the literature. Therefore, until a better explanation can be found we consider the electrical (ephaptic) mechanism as most likely for this novel type of retrograde communication characterized by supralinear changes in the amplitudes of minimal EPSPs with postsynaptic hyperpolarization.

Acknowledgements

We thank Drs A. Nistri and M. Volgushev for helpful comments, W.W. Anderson and A.V. Astrelin for programming and M. Diamond for reading the manuscript. This work was supported by Ministero dell'Universita' e Ricerca Scientifica e Tecnologica (E.C.), Volkswagen Foundation, INTAS and Russian Foundation for Basic Research (L.L.V.). N.B. was supported by a NOVARTIS Pharma fellowship.

References

Astrelin, A.V., Sokolov, M.V., Behnisch, T., Reymann, K.G., Voronin, L.L., 1998. Principal components analysis of minimal excitatory postsynaptic potentials. Journal of Neuroscience Methods 79, 169–186.

Berretta, N., Rossokhin, A.V., Cherubini, E., Astrelin, A.V., Voronin, L.L., 1999. Long-term synaptic changes induced by intracellular tetanization of CA3 pyramidal neurons in hippocampal slices from juvenile rat. Neuroscience 93, 469–477.

Bliss, T.V.P., Collingridge, G.L., 1993. A synaptic model for memory: long-term potentiation in the hippocampus. Nature 361, 31–39.

Bradler, J.E., Barrionuevo, G., 1990. Heterosynaptic correlates of long-term potentiation induction in hippocampal CA3 neurons. Neuroscience 35, 265–271.

Byrne, J.H., Kandel, E.R., 1996. Presynaptic facilitation revisited: state and time dependence. Journal of Neuroscience 16, 425–435.

Byzov, A.L., Shura-Bura, T.M., 1986. Electrical feedback mechanism in the processing of signals in the outer plexiform layer of the retina. Vision Research 26, 33–34.

Calverley, R.K.S., Jones, D.G., 1990. Contributions of dendritic spines and perforated synapses to synaptic plasticity. Brain Research Reviews 15, 215–249.

Claiborne, B.J., Amaral, D.J., Cowan, W.M., 1986. A light and electron microscopic analysis of the mossy fibers of the rat dentate gyrus. Journal of Comparative Neurology 246, 435–458.

Clark, K.A., Randall, A.D., Collingridge, G.L., 1994. A comparison of paired-pulse facilitation of AMPA and NMDA receptor-mediated excitatory postsynaptic currents in the hippocampus. Experimental Brain Research 104, 272–278.

Dobrunz, L.E., Huang, E.P., Stevens, C.F., 1997. Very short-term plasticity in hippocampal synapses. Proceedings of the National Academy of Sciences, USA 94, 14843–14847.

Durand, G.M., Kovalchuk, Y., Konnerth, A., 1996. Long-term potentiation and functional synapse induction in developing hippocampus. Nature 381, 71–75.

Edwards, F.A., 1995. Anatomy and electrophysiology of fast central synapses lead to structural model for long-term potentiation. Physiological Review 75, 759–787.

Faber, D.S., Korn, H., 1991. Application of the coefficient of variation methods for analyzing synaptic plasticity. Biophysics Journal 60, 1288–1294.

Fitzsimond, R.M., Poo, M.-M., 1998. Retrograde signaling in the development and modification of synapses. Physiological Review 78, 143–170.

Glitsch, M., Llano, I., Marty, A., 1996. Glutamate as a candidate retrograde messenger at interneurone-Purkinje cell synapses of rat cerebellum. Journal of Physiology, London 497, 531–537.

Henze, D.A., Card, J.P., Barrionuevo, G., Ben-Ari, Y., 1997. Large amplitude miniature excitatory postsynaptic currents in hippocampal CA3 pyramidal neurons are of mossy fiber origin. Journal of Neurophysiology 77, 1075–1086.

Huguenard, J.R., 1996. Low-threshold calcium currents in central nervous system neurons. Annual Review of Physiology 58, 329–348.

Isaac, J.T.R., Nicoll, R.A., Malenka, R.C., 1995. Evidence for silent synapses: implications for the expression of LTP. Neuron 16, 427–434.

Jackson, M.B., Konnerth, A., Augustine, G.J., 1991. Action potential broading and frequency-dependent facilitation of calcium signals in pituitary nerve terminals. Proceedings of the National Academy of Sciences, USA 88, 380–384.

Johnston, D., Williams, S., Jaffe, D., Gray, R., 1992. NMDA-receptor independent long-term potentiation. Annual Review of Physiology 54, 489–505.

Jonas, P., Burnashev, N., 1995. Molecular mechanisms controlling calcium entry through AMPA-type glutamate receptor channels. Neuron 15, 987–990.

Jonas, P., Major, G., Sakmann, B., 1993. Quantal components of unitary EPSCs at the mossy fibre synapse on CA3 pyramidal cells of rat hippocampus. Journal of Physiology, London 472, 615–663.

Kamiya, H., Shinozaki, H., Yamamoto, C., 1996. Activation of metabotropic glutamate receptor type 2/3 suppresses transmission at rat

hippocampal mossy fiber synapses. Journal of Physiology, London 493, 447–455.
Katz, B., 1969. The Release of Neural Transmitter Substance. Charles C. Thomas, Springfield, Illinois.
Korn, H., Bausela, F., Charpier, S., Faber, D.S., 1993. Synaptic noise and multiquantal release at dendritic synapses. Journal of Neurophysiology 70, 1249–1254.
Larkman, A.U., Jack, J.J., Stratford, K.J., 1997. Quantal analysis of excitatory synapses in rat hippocampal CA1 in vitro during low-frequency depression. Journal of Physiology, London 505, 457–471.
Maccaferri, G., Mangoni, M., Lazzari, A., DiFrancesco, D., 1993. Properties of the hyperpolarization-activated current in rat hippocampal CA1 pyramidal cells. Journal of Neurophysiology 69, 2129–2136.
Markram, H., Sakmann, B., 1994. Calcium transients in dendrites of neocortical neurons evoked by single subthreshold excitatory postsynaptic potentials via low-voltage-activated calcium channels. Proceedings of the National Academy of Sciences, USA 91, 5207–5211.
Muller, D., 1997. Ultrastructural plasticity of excitatory synapses. Reviews in Neuroscience 8, 77–93.
Sabatini, B.L., Regehr, W.G., 1999. Timing of synaptic transmission. Annual Review of Physiology 61, 521–542.
Sokolov, M.V., Rossokhin, A.V., Behnisch, T., Reymann, K.G., Voronin, L.L., 1998. Interaction between paired-pulse facilitation and long-term potentiation of minimal EPSPs in rat hippocampal slices: a patch clamp study. Neuroscience 85, 1–13.
Spruston, N., Jaffe, D., Johnston, D., 1994. Dendritic attenuation of synaptic potentials and currents: the role of passive membrane properties. Trends in Neuroscience 17, 161–166.
Spruston, N., Jonas, P., Sakmann, B., 1996. Dendritic glutamate receptor channels in rat hippocampal CA3 and CA1 pyramidal neurons. Journal of Physiology, London 482, 325–352.
Stratford, K.J., Tarczy-Hornoch, K., Martin, K.A., Bannister, N.J., Jack, J.J.B., 1996. Excitatory synaptic inputs to spiny stellate cells in cat visual cortex. Nature 382, 258–262.
Takeuchi, A., Takeuchi, N., 1961. Changes in potassium concentration around motor nerve terminals, produced by current flow, and their effects on neuromuscular transmission. Journal of Physiology, London 155, 46–58.
Urban, N.N., Barrionuevo, G., 1998. Active summation of excitatory postsynaptic potentials in hippocampal CA3 pyramidal neurons. Proceedings of the National Academy of Sciences, USA 95, 11450–11455.
Volgushev, M., Voronin, L.L., Chistiakova, M., Artola, A., Singer, W., 1995. All-or-none excitatory postsynaptic potentials in the rat visual cortex. European Journal of Neuroscience 7, 1751–1760.
Voronin, L.L., 1993. On the quantal analysis of hippocampal long-term potentiation and related phenomena of synaptic plasticity. Neuroscience 56, 275–304.
Voronin, L.L., Kuhnt, U., Gusev, A.G., Hess, G., 1992. Quantal analysis of long-term potentiation of "minimal" excitatory postsynaptic potentials in guinea pig hippocampal slices: binomial approach. Experimental Brain Research 89, 275–287.
Voronin, L., Byzov, A., Kleschevnikov, A., Kozhemyakin, M., Kuhnt, U., Volgushev, M., 1995. Neurophysiological analysis of long-term potentiation in mammalian brain. Behavioral Brain Research 66, 45–52.
Voronin, L.L., Volgushev, M., Sokolov, M., Kasyanov, A., Chistiakova, M., Reymann, K.G., 1999. Evidence for an electrical feedback in cortical synapses: postsynaptic hyperpolarization alters the number of response failures and quantal content. Neuroscience 92, 399–405.
Wall, M.J., Usowicz, M.M., 1998. Development of the quantal properties of evoked and spontaneous synaptic currents at a brain synapse. Nature Neuroscience 1, 675–683.
Wang, J.-H., Kelly, P.T., 1996. Regulation of synaptic facilitation by postsynaptic Ca^{2+}/CaM pathways in hippocampal CA1 neurons. Journal of Neurophysiology 76, 276–286.
Winslow, J.L., Duffy, S.N., Charlton, M.P., 1994. Homosynaptic facilitation of transmitter release in crayfish is not affected by mobile calcium chelators: implications for the residual ionized calcium hypothesis from electrophysiological and computational analyses. Journal of Neurophysiology 72, 1769–1793.
Wu, L.-G., Saggau, P., 1997. Presynaptic inhibition of elicited neurotransmitter release. Trends in Neuroscience 20, 204–212.